

Age-dependent remodelling of ionotropic signalling in cortical astroglia

Ulyana Lalo,¹ Oleg Palygin,² Richard Alan North,³ Alexei Verkhratsky^{3,4} and Yuriy Pankratov²

¹Cell Physiology and Pharmacology, University of Leicester, Leicester LE1 9HN, UK

²Department of Biological Sciences, University of Warwick, Coventry, CV4 7AL, UK

³Faculty of Life Sciences, The University of Manchester, Manchester M13 9PT, UK

⁴Institute of Experimental Medicine, ASCR, Videnska 1083, 142 20 Prague 4, Czech Republic

Summary

Cortical astrocytes express fast ionotropic receptors for glutamate and ATP, although their role in neurone–glia communication remains controversial. Stimulation of neuronal afferents in mice neocortex triggers complex glial synaptic currents (GSCs) mediated by NMDA, P2X and AMPA receptors and glutamate transporters. In addition, astrocytes demonstrate spontaneous ‘miniature’ GSCs resulting from quantal release of neurotransmitters. Here, we demonstrate that maturation and aging of the brain of mice (from 1 to 21 months) affect the density of ionotropic receptors in astrocytes and their role in GSCs generation. The AMPA-receptor-mediated component is the largest in young animals and progressively declines with age. The P2X and NMDA components of GSC are smallest in young, maximal in adult (3 and 6 months old) and once more decrease in old mice, probably reflecting the remodelling of neuronal–glial circuitry. Our results demonstrate that fast synaptic transmission between neurones and astrocytes in neocortex that may be involved in information processing in neuronal–glial networks undergoes remodelling during brain maturation and aging.

Key words: astrocytes; aging; synaptic transmission; AMPA receptors; NMDA receptors; P2X receptors.

Correspondence

Professor Alexei Verkhratsky, Faculty of Life Sciences, The University of Manchester, Smith Building, Oxford Road, Manchester M13 9PT, UK.
Tel.: (+44 161) 2755414; e-mail: Alexei.Verkhatsky@manchester.ac.uk

or

Dr Yuriy Pankratov, Department of Biological Sciences, University of Warwick, Coventry, CV4 7AL, UK. Tel.: (+44 247) 6528373; fax: (+44 247) 6523701; e-mail: Y.Pankratov@warwick.ac.uk

Accepted for publication 28 December 2010

Introduction

The development and aging of the brain is associated with remodelling of synaptic contacts and plastic changes in neural networks. The formation, maintenance and modification of these networks depend on the interaction between neurones and neuroglia. It is now universally acknowledged that glial cells express an extensive complement of neurotransmitter receptors that can be activated during synaptic transmission in the CNS (Verkhratsky *et al.*, 1998; Volterra & Meldolesi, 2005; Fellin *et al.*, 2006; Haydon & Carmignoto, 2006). According to the ‘tripartite’ architecture of CNS synapses (Araque *et al.*, 1999; Bezzi *et al.*, 2001; Haydon, 2001; Halassa *et al.*, 2007), parts of astroglial membranes are located in close vicinity to neurotransmitter release sites. Ionotropic receptors located in such areas may therefore mediate evoked and spontaneous currents similar to those observed in neurones (Bergles *et al.*, 2000; Lalo *et al.*, 2006). Membrane physiology of maturing and aging astrocytes is virtually unexplored. All information about active neuronal–glial connections has been derived from the experiments on newborn or young animals, whereas the age-dependent modification of these connections remains unknown.

Our previous analysis of cortical astrocytes revealed functional expression of NMDA receptors as well as AMPA and P2X_{1/5} receptors; unusually, the NMDA receptors showed no Mg²⁺ block (Lalo *et al.*, 2006, 2008). These ionotropic receptors can be activated by release of glutamate and ATP from cortical synaptic terminals (Pankratov *et al.*, 2007) at physiological membrane potentials. Here, we report in-depth analysis of the age-dependent changes in synaptically activated responses in astroglia which we performed trying to understand how maturation of the brain affects signalling in neuronal–glial circuitry.

Materials and methods

Neocortical slice preparation

Experiments were performed on somato-sensory cortex isolated from the brains of transgenic mice expressing enhanced green fluorescent protein (EGFP) under the control of the human glial fibrillary acidic protein (GFAP) promoter (line TgN(GFAP-EGFP) GFEC-FKi; see (Nolte *et al.*, 2001; Matthias *et al.*, 2003; Grass *et al.*, 2004; Lalo *et al.*, 2008)). Mice (1–21 months old) were anaesthetized by halothane and then decapitated, in accordance with UK legislation. Slices were prepared using the technique described previously (Lalo *et al.*, 2006). Brains were rapidly dissected and placed in physiological saline containing (in

mm): 135 NaCl, 3 KCl, 1 MgCl₂, 2.4 CaCl₂, 26 NaHCO₃, 1 NaH₂PO₄, 15 glucose, pH 7.4 when gassed with 95% O₂/5% CO₂. Cortical slices (280–300 µm thick) were cut at 4°C and kept at room temperature for 1–2 h prior the cell isolation.

Acute isolation of astrocytes

Astrocytes were acutely isolated using the modified 'vibrating ball' technique (Pankratov *et al.*, 2002; Lalo *et al.*, 2006). The glass ball (200 µm diameter) was moved slowly some 10–50 µm above the slice surface, while vibrating at 100 Hz (lateral displacements 20–30 µm). The composition of external solution for isolated cell experiments was (mm) 135 NaCl; 2.7 KCl; 2.5 CaCl₂; 1 MgCl₂; 10 HEPES, 1 NaH₂PO₄, 15 glucose, pH adjusted with NaOH to 7.3.

Identification of astrocytes

Astrocytes were identified by EGFP fluorescence. For this purpose, cells were illuminated at 488 nm and observed at 515 ± 10 nm. Visually identified cells demonstrated electrophysiological signature characteristic of astrocytes (e.g. low input resistance, lack of fast time-dependent conductances, Fig. 1).

Electrophysiological recordings

Whole-cell voltage-clamp recordings from isolated astrocytes and astrocytes *in situ* were made with patch pipettes (5–6 MΩ) filled with intracellular solution (in mm): 110 KCl, 10 NaCl, 10 HEPES, 5 MgATP, 0.2 EGTA, pH 7.35. The membrane potential was clamped at –80 mV unless stated otherwise. Currents were monitored using an AxoPatch200B patch-clamp amplifier (Axon Instruments-Molecular Devices, Austin, TX, USA) filtered at 2 kHz and digitized at 4 kHz. Experiments were controlled by PCI-6229 data acquisition board (National Instruments, Austin, TX, USA) and WinFluor software (Strathclyde Electrophysiology Software; Strathclyde, UK); data were analysed by self-designed software.

Liquid junction potentials were measured with the patch-clamp amplifier; all voltages reported were corrected accordingly. Recordings commenced 10 min after whole-cell access was gained, to ensure equilibration between the pipette solution and the cytosol. Series resistances were 5–12 MΩ and input resistances were 50–150 MΩ; both varied by < 20% in the cells accepted for analysis. A modified 'square-pulse' concentration jump method (Lalo *et al.*, 2001; Pankratov *et al.*, 2002) was used for rapid (exchange time ~5 ms) applications of solutions containing various agents to single cells. Antagonists of ATP and glutamate receptors (PPADS, D-AP5 and CNQX) were pre-applied for 2 min before application of agonists.

In situ recordings

Whole-cell voltage-clamp recordings were made from identified astrocytes situated in the layer II of somato-sensory cortex. All

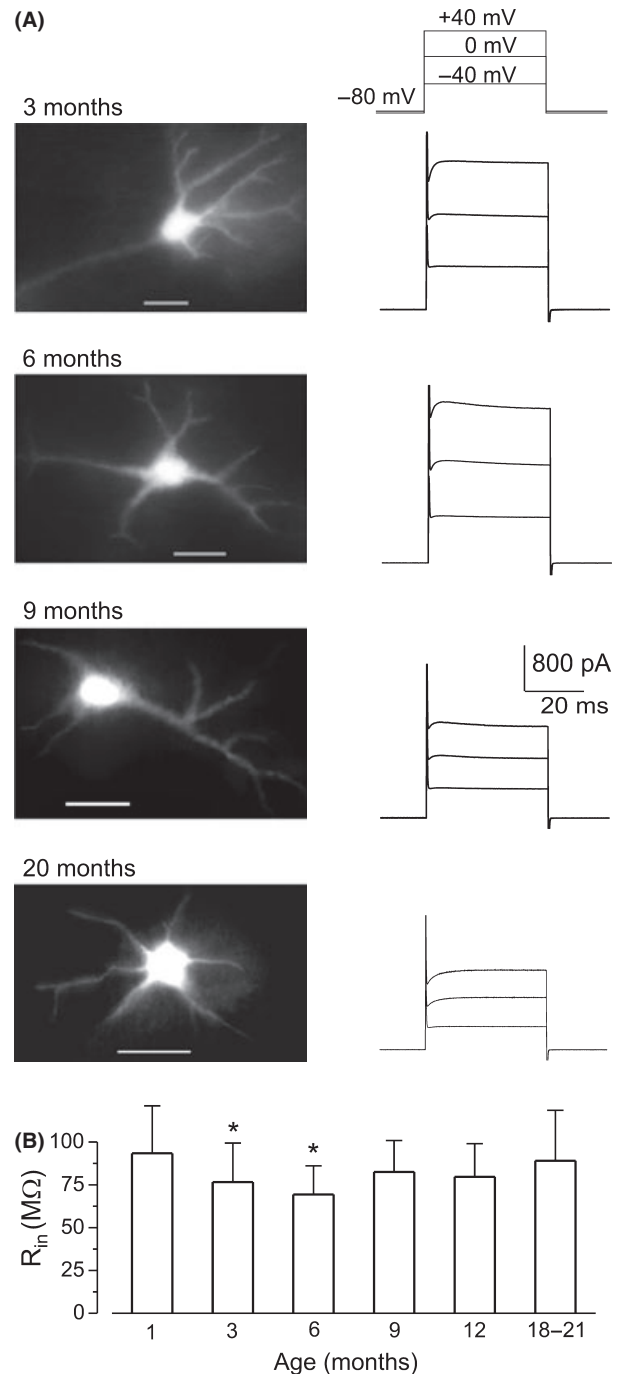


Fig. 1 Identification and basic electrophysiological properties of cortical astrocytes *in situ*. (A) Representative enhanced green fluorescent protein images (left column) of cortical layer II astrocytes of different age groups and corresponding whole-cell currents (right column) evoked to depolarizing steps from the holding potential of –80 mV; the voltage protocol is shown on the top. (B) Age-related changes in the input resistance of cortical astrocytes. Data are presented as mean ± SD for 15 cells in the each age group; decrease in the astrocyte R_{in} measured in three and 6 months in comparison with 1 month was statistically significant with $P < 0.05$ (one-way ANOVA).

recordings shown were made at temperature of 30–32°C in the presence of 100 µM picrotoxin, and membrane potential was kept at –80 mV unless specifically indicated. Axons originating

from layer IV–VI neurones were stimulated at 0.25–1.0 Hz with a bipolar coaxial electrode (WPI, Stevenage, UK) placed in the layer IV approximately opposite to the site of recording; stimulus duration was 300 μ s. The stimulus magnitude was set 3–4 times higher than minimal stimulus adjusted to activate the single-axon response in the layer II pyramidal neurons as described by (Pankratov *et al.*, 2007). At such stimulus magnitude (further referred as moderate, typically 2.5–5 μ A), neuronal excitatory postsynaptic currents (EPSCs) were 3–5 times higher than those evoked by minimal stimulation, but still exhibited large amplitude fluctuations with failures in 10–15% of trials. Thus, one could expect that just a few intra-cortical axons and limited number of synapses were activated at chosen stimulus intensity.

The currents evoked in the layer II astrocytes by moderate stimulus exhibited large amplitude fluctuations, their average amplitude reached 15–30% of maximal current evoked by saturating stimulus (30–40 μ A); no noticeable astroglial response was recorded at stimulus intensity below minimal (i.e. threshold intensity for neuronal EPSCs).

Fluorescent Ca^{2+} imaging

To monitor the cytoplasmic free Ca^{2+} concentration ($[\text{Ca}^{2+}]_i$), cortical astrocytes were loaded with 100 μ M Fura-2 (Ca^{2+} probe equimolarly substituting EGTA in the intracellular saline) through the patch pipette in whole-cell configuration. For fura-2 excitation, cells were alternately illuminated at wavelengths 340 ± 5 nm and 380 ± 5 nm using OptoScan monochromator (Cairn, Faversham, UK); emission was collected at 515 ± 10 nm. Fluorescent images were recorded using Olympus BX51 microscope equipped with UMPLFL20x/NA0.95 objective and $2 \times$ intermediate magnification and Andor iXon885 EMCCD camera; exposure time was 35 ms at 2×2 binning. Astrocyte whole-cell currents were recorded simultaneously; experiments were controlled by WinFluor software (Strathclyde Electrophysiology Software; Glasgow, UK). The $[\text{Ca}^{2+}]_i$ levels were expressed as F_{340}/F_{380} ratio after background subtraction. To quantify the average amplitude of Ca^{2+} transients in different age groups, the F_{340}/F_{380} ratios were averaged over the whole-cell image over two 1s-long time windows, in the rest (immediately before stimulus) and at the peak of transient; after then, the resting F_{340}/F_{380} value was subtracted from the peak value.

Pharmacological isolation of different components of glial currents

To functionally characterize the components of glial currents activated by synaptic stimulation, cortical slices were treated with the following pharmacological agents: (i) a combination of the antagonists of glutamate transporters (3S)-3-[[[3-[[4-(trifluoromethyl)benzoyl]amino]phenyl]methoxy]-L-aspartic acid (TFB-TBOA), 1 μ M and DL-threo-b-benzyloxyaspartic acid (DL-TBOA), 30 μ M [this mixture, referred to as TBOA-mix, blocks excitatory amino-acid transporters of EAAT1–5 types, some of which

(EAAT1/2) are expressed in astroglia (Danbolt, 2001; Hu *et al.*, 2003)]; (ii) a selective antagonist of AMPA receptors, 6-Cyano-7-nitroquinoxaline-2,3-dione (CNQX), 50 μ M; (iii) a selective antagonist of NMDA receptors, D-(-)-2-Amino-5-phosphonopentanoic acid (D-AP5), 30 μ M; and (iv) the P2X receptor antagonist pyridoxal-phosphate-6-azophenyl-2',4'-disulfonic acid tetrasodium salt (PPADS), 10 μ M. In some experiments, we also used a selective P2X_{1/5} inhibitor NF449 at 10 nM concentration (Rettinger *et al.*, 2005). According to our previous reports (Lalo *et al.*, 2006, 2008), these concentrations of antagonists effectively inhibited P2X and glutamate receptors expressed in the cortical astrocytes.

Data analysis

All data are presented as mean \pm SD, the statistical significance of difference between age groups was tested by one-way ANOVA test, unless indicated otherwise. The synaptically evoked and spontaneous astroglial transmembrane currents were analysed off-line using methods described by Pankratov & Krishtal (2003; Pankratov *et al.* (2007). Briefly, preliminary evaluation of the amplitude bi-phasic glial synaptic currents (GSCs) was made by averaging the amplitude of GSC in 1-msec time window at peak (I_{peak}) and 200 ms after peak (I_{200}). After that, each GSC was fitted with two model curves (e.g. 'fast' and 'slow' components), and each model curve had mono-exponential rise and decay phases. The decay time constant of fast component was varying in the range of 10–50 ms, while decay time constant of slow component varied between 400 ms and 2.5 s; such difference in the kinetics ensured unambiguous separation of components. The minimal square root procedure was used to determine the amplitude of the model curves, while the time constants and offset were optimized by the gradient method to minimize the mean square error. For the initial detection of spontaneous events, the inward transmembrane currents of amplitude higher than 2 SD of baseline noise were selected. After then, every single spontaneous event was analysed within the 140-ms time window, and its amplitude and kinetics were determined by fitting the model curve with single exponential rise and decay phases. As a rule, mean square error of fit amounted to 5–15% of peak amplitude for the GSCs and 5–20% for the spontaneous currents, depending on the background noise. Whenever error of fit exceeded 25%, spontaneous currents were discarded from further analysis. The amplitude distributions of spontaneous and evoked currents were analysed with the aid of probability density functions and likelihood maximization techniques, as described by Stricker *et al.* (1996) and Pankratov & Krishtal (2003); all histograms shown were calculated as density functions.

Drugs

Receptor antagonists were from Tocris (Bristol, UK). Other salts and chemicals were from Sigma (Dorset, UK) unless specifically indicated.

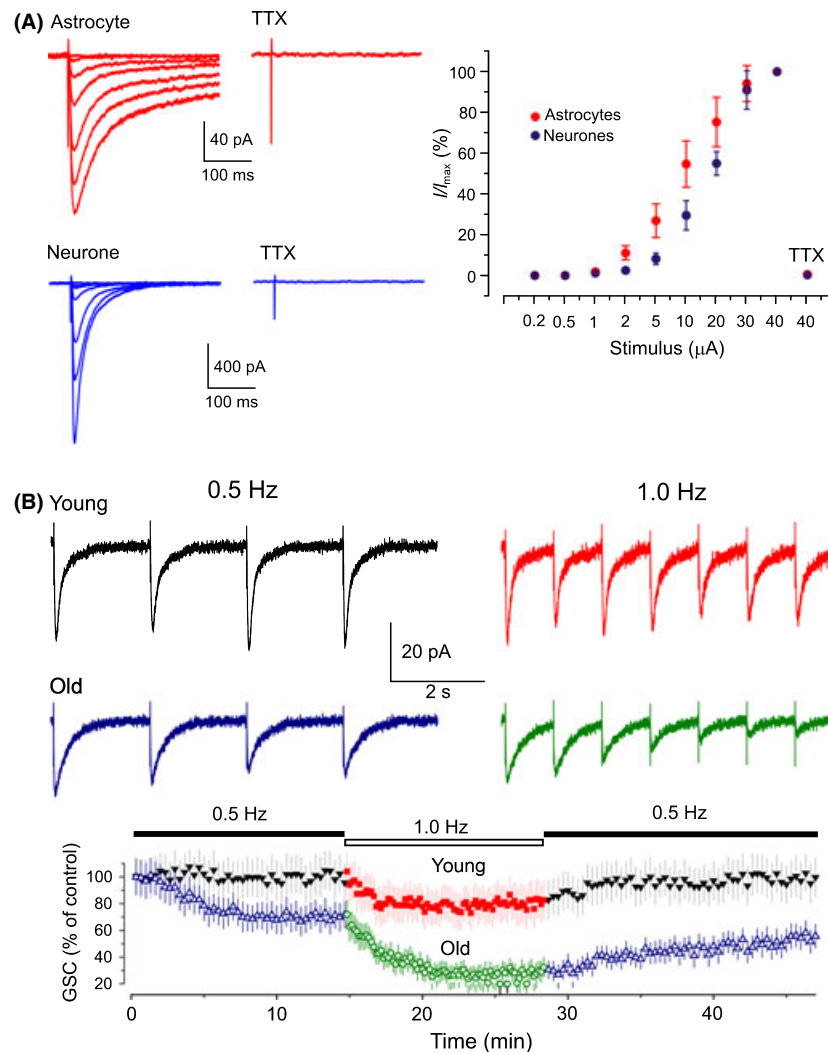


Fig. 2 General functional properties of glial synaptic currents (GSC) *in situ* in cortical slices. (A) Stimulus dependence and tetrodotoxin (TTX) sensitivity of GSC. Left panel shown synaptic current recorded separately in astrocyte and neurone in the same cortical slice at different stimulation amplitudes (1, 2, 5, 10, 20, 30 and 40 μ A). The mean \pm SD values of normalised amplitudes of astroglial/neuronal synaptic currents are shown on the graph (right panel); data are shown for five astrocytes and seven neurones from 6- to 10-week-old mice. Incubation with 1 μ M of TTX completely abolished both neuronal and astroglial responses. (B) Frequency-dependence of GSC. The glial responses were reliably evoked for 40–60 min at stimulation frequency of 0.5 Hz, and increasing of stimulation frequency to 1.0 Hz causes only minor decrease in the GSC amplitude in the young (3 and 6 months old) animals but causes considerable decrease the GSCs recorded in the old (12–20 months) mice. Representative current traces are shown on the top. The bottom plot shows changes in the GSCs amplitude quantified for five astrocytes for each group; normalized amplitudes of glial currents (mean \pm SD for five cells) are plotted vs. recording time. Each point represents the average amplitude (relative to control) of ten sequential currents.

Results

Membrane properties of astrocytes in different age groups

We performed voltage-clamp recordings from protoplasmic astrocytes in layer II of somato-sensory cortex of EFGP/GFAP mice (Nolte *et al.*, 2001) of six different age groups of: 1, 3, 6, 9, 12 and 18–21 months of age. The astrocytes in acutely isolated slices were identified by green fluorescence and by their characteristic electrophysiological signature (Fig. 1A). Aging did not affect resting potential of astroglial cells (V_{mem} values were -81.2 ± 1.6 mV, -82.7 ± 2.4 mV, -83.5 ± 2.9 , -81.4 ± 1.7 mV,

$n = 7$ for 1, 3, 6 and 9 months old animals, respectively, and -81.3 ± 2.1 and 80.9 ± 2.6 mV, $n = 5$ for 12 and 18–21 months old groups, respectively). Similarly, we have not observed significant changes in membrane current pattern in astrocytes of different ages. Instead, we detected a small (~ 20 –30%) yet statistically significant decrease in the input resistance of astrocytes in the three- and 6-months-old mice (Fig. 1B).

Age-dependent changes in evoked synaptic currents

We confirmed our previous observations (Lalo *et al.*, 2006) that stimulation of neuronal afferents originating from layers IV–VI induced complex ion currents in astrocytes (Figs 2 and 3). These

currents were directly associated with synaptic transmission because (i) treatment of slices with 1 μM TTX completely abolished glial responses (Fig. 2A), (ii) the amplitude of the glial response was stimulus-dependent in a manner similar to the synaptic current evoked in the neighbouring neurones (Fig. 2A) and (iii) glial postsynaptic currents could be recorded for a long time at frequencies 0.5 Hz, this demonstrating frequency-dependence was similar to neuronal EPSCs (Fig. 2B). Therefore, we identified astroglial responses as GSCs; the GSCs were recorded in all age groups. The maximal amplitude of astrocytic response to the synaptic stimulation ranged between 20 and 200 pA depending on the age, the amplitude of GSC evoked by moderate stimulus varied typically between 5 and 60 pA. The GSCs recorded from the astrocytes of old mice (12 and 18–21 months old) were markedly depressed in the course of repetitive stimulation, whereas amplitude of GSCs in younger animals (1–6 months) was stable at high (1 Hz) stimulation frequency (Fig. 2B).

The GSCs recorded in astrocytes had complex kinetics, with fast and slow components. Fast component of GSCs had a decay time $\tau_{\text{fast}} = 27.2 \pm 8.8$ ms, whereas the slow component of GSCs decayed with $\tau_{\text{slow}} = 1.4 \pm 0.8$ s ($n = 38$). The antagonists, applied in appropriate concentrations to block glutamate transporters (TBOA-mix) and astroglial ionotropic receptors (CNQX, D-AP5 and PPADS), inhibited both peak (I_{peak}) and delayed ($I_{200\text{ms}}$) components of GSC (Fig. 3). Effects of antagonists were reversible, and the GSC amplitude gradually recovered after washout. In the presence of all antagonists, GSCs were blocked almost completely (by 95–99%; $n = 38$), indicating that GSCs were mediated primarily by ATP and glutamate receptors and glutamate transporters. The small (1–5%) residual component of GSC may be associated with redistribution of potassium in the vicinity of astrocytic membrane. This pharmacological profile confirmed our previous findings of the role for AMPA and NMDA glutamate receptors in generation of astroglial synaptic currents (Lalo *et al.*, 2006), and demonstrated the involvement of P2X receptors (Lalo *et al.*, 2008) in shaping synaptically activated astroglial currents.

The glial synaptic responses demonstrated age-dependent remodelling. First, the average amplitude of synaptic response activated by moderate stimulus strength increased significantly after 1 month attaining highest levels (35–50 pA) in mature adult (3 and 6 months) animals; it declined again at more advanced (9–21 months) age to the lowest level of 5–10 pA measured in old (18–21 months) group (Fig. 3C). The maximal amplitude of synaptic response was changed the similar pattern accordingly, with highest level (180–240 pA) in the mature adult and lowest level (15–25 pA) in the old animals (data not shown). Second, aging affected the relative weight of fast and slow components of GSCs (Fig. 3C). The relative contribution of the fast component was the lowest at 1 month of age, became predominant in young adults (3 and 6 months), and declined at advanced age (9–21 months). Third, the changes in GSCs kinetics reflected age-dependent changes in their pharmacological

profiles, thus indicating changes in the underlying molecular machinery (Fig. 3D).

The contribution of P2X receptors to GSCs was higher in younger ages, reaching maximal values of $56 \pm 6\%$ (fast component) and $39 \pm 4\%$ (slow component) at 3 months ($n = 9$). In contrast, the contribution of NMDA receptors grew steadily with age, being maximal at 9–21 months for the fast component ($53 \pm 6\%$, $n = 10$) and at 6 months for the slow component ($53 \pm 7\%$, $n = 9$); at the older ages, contribution of NMDA component slightly declined. AMPA receptors contributed exclusively to the fast component of GSCs, their contribution was maximal at 1 month ($18 \pm 4\%$, $n = 10$) and sharply declined at older ages. The contribution of glutamate transporters to GSCs was minimal in 3 months, but increased again at 9–21 months.

Age-dependent changes in spontaneous synaptic currents

Similarly to our previous reports (Lalo *et al.*, 2006), we observed spontaneous 'miniature' glial synaptic currents (mGSCs) in the presence of Na^+ -channel blocker tetrodotoxin (1 μM) and GABA receptor antagonist picrotoxin (100 μM) at holding potential -80 mV in astrocytes of all age groups (Fig. 4). Analysis of the spontaneous events revealed two distinct groups of mGSCs with different decay kinetics. Fast mGSCs had an amplitude in the range of 5–10 pA and a decay time of 10.8 ± 2.9 ms; slow mGSCs amplitudes varied between 5 and 25 pA, and a decay time was 28.5 ± 11.2 ms ($n = 46$). Depending on the age of animals, the amplitude ratio of fast to slow mGSCs was in the range of 0.55–0.85, the relative frequency of fast mGSCs was 40–60% of the total.

The mGSCs were insensitive to TBOA-mix but were differentially inhibited by antagonists of glutamate and P2X receptors. Inhibition of the AMPA receptors with 50 μM CNQX did not affect the fast mGSCs (Fig. 4), although it somewhat reduced the amplitude of slow mGSCs by $23 \pm 11\%$ ($n = 41$, all ages) without affecting their frequency.

In the presence of CNQX, the time of decay of slow mGSCs was slightly increased ($13 \pm 9\%$, $n = 41$). Subsequent (i.e. in the presence of CNQX) inhibition of NMDA receptors by D-AP5 eliminated slow currents in all cells leaving the fast mGSCs intact (Fig. 4A,B). In contrast to glutamate receptor antagonists, application of PPADS did not affect the slow mGSCs but significantly inhibited fast currents (Fig. 4A,B). On average 10 μM PPADS decreased the amplitude and frequency of fast mGSCs by 67 ± 12 and $82 \pm 15\%$ ($n = 37$), respectively. Therefore, cortical astrocytes demonstrate two distinct populations of spontaneous currents: fast mGSCs mediated by P2X receptors and slow glutamatergic mGSCs mediated mainly by NMDA receptors with minor contribution of AMPA receptors.

The unitary size of purinergic and glutamatergic mGSCs was evaluated through the corresponding peaks in the amplitude histograms. The unitary size of P2X receptor-mediated mGSCs varied in an age-dependent manner between 2.8 and 7.5 pA,

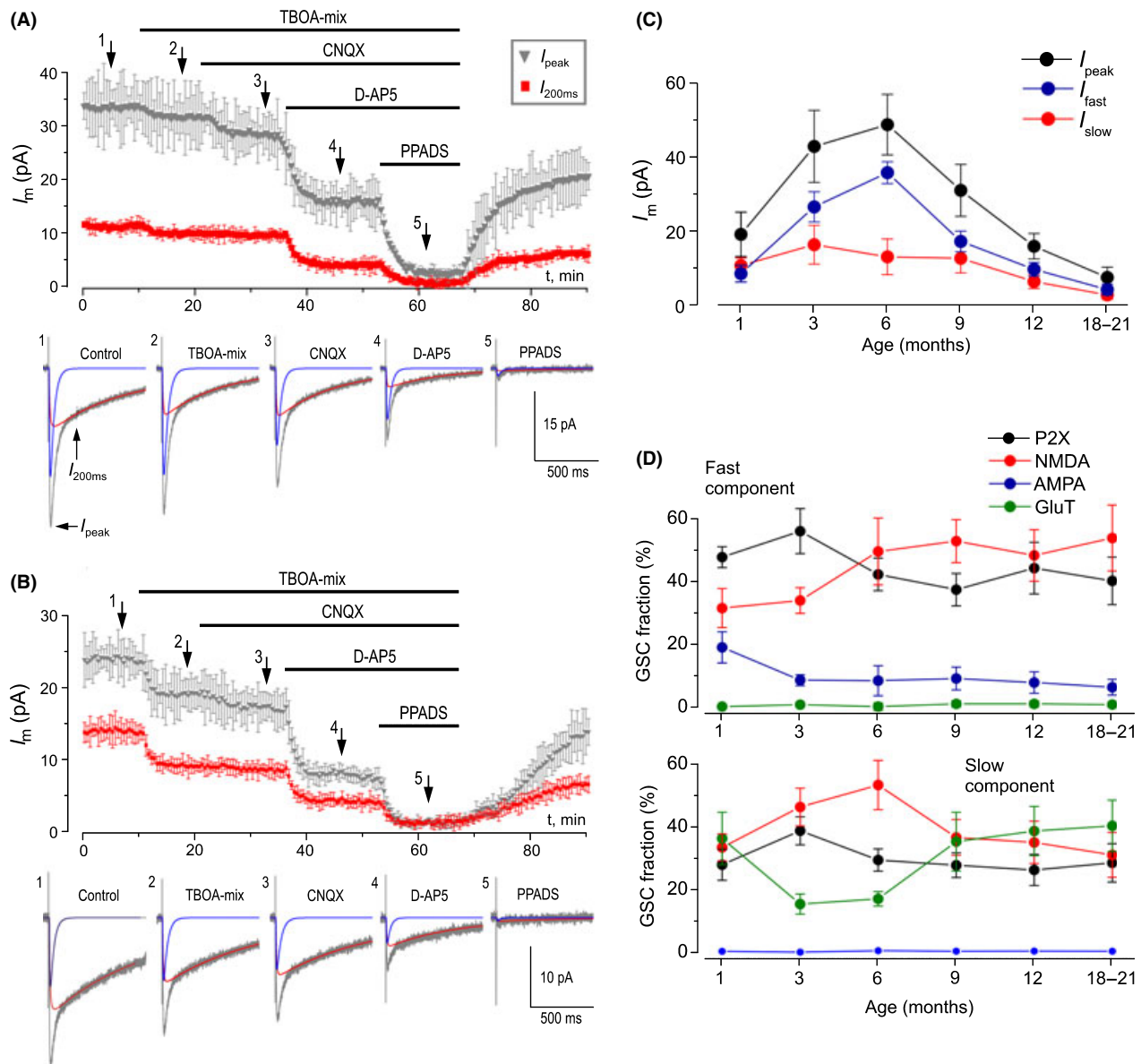


Fig. 3 Synaptic currents in astrocytes in acutely isolated cortical slices. (A, B) Transmembrane currents evoked in the astrocytes in neocortical layer II of 3-month-old (A) and 9-month-old (B) mice *in situ* by moderate stimulation of neuronal afferents were recorded at membrane potential of -80 mV in the presence of $100 \mu\text{M}$ picrotoxin. The glial synaptically activated currents (GSCs) were inhibited by consecutive application of mixture of $1 \mu\text{M}$ TFB-TBOA and $30 \mu\text{M}$ DL-TBOA, $50 \mu\text{M}$ CNQX, $30 \mu\text{M}$ D-AP5 and $10 \mu\text{M}$ PPADS. Amplitudes of GSC were monitored at peak (I_{peak} , grey dots) and 200 after peak (I_{200} , red dots) when only slow component remained. Each point on the time graphs represents the mean \pm SD for five GSCs; examples of GSCs traces and corresponding fast (blue line) and slow (red line) components are shown below. Note the difference in the shape and pharmacological sensitivity of GSC recorded in mice of different age. (C) Age-dependent changes in peak amplitude of total synaptic current (black), of the fast (blue) and slow (red) components of GSC evoked the cortical astrocytes by the moderate stimulation of neuronal afferents; amplitude of fast and slow components were determined by fitting two model curves as shown in (A, B) and described in the Methods. (D) Pharmacological profile of fast and slow components of evoked GSCs in mice of different ages. The data, presented as mean \pm SD for 6–10 cells for each age group, were calculated from the inhibitory effect of the appropriate agonist.

whereas the unitary size of NMDA receptor-mediated mGSCs varied between 3.4 and 10.3 pA (Fig. 4D). Importantly, unitary size of purinergic and glutamatergic mGSCs correlated with quantal size of corresponding fraction of fast evoked GSCs at all ages, as discussed below.

The differences in the properties of the fast and slow components of GSCs may indicate that they are generated at the different parts of astroglial membrane. The fast component mediated

mostly by ionotropic receptors [including AMPA receptors (Lalo *et al.*, 2006)] with low affinity to glutamate) could be generated in areas exposed to the rapid transients of high concentrations of glutamate. These areas of astroglial membranes are located close to the release sites and may even protrude into the synaptic cleft (Verkhratsky & Kirchhoff, 2007). In contrast, the slow GSC component has a significant contribution to glutamate transporter-mediated current and therefore may originate from

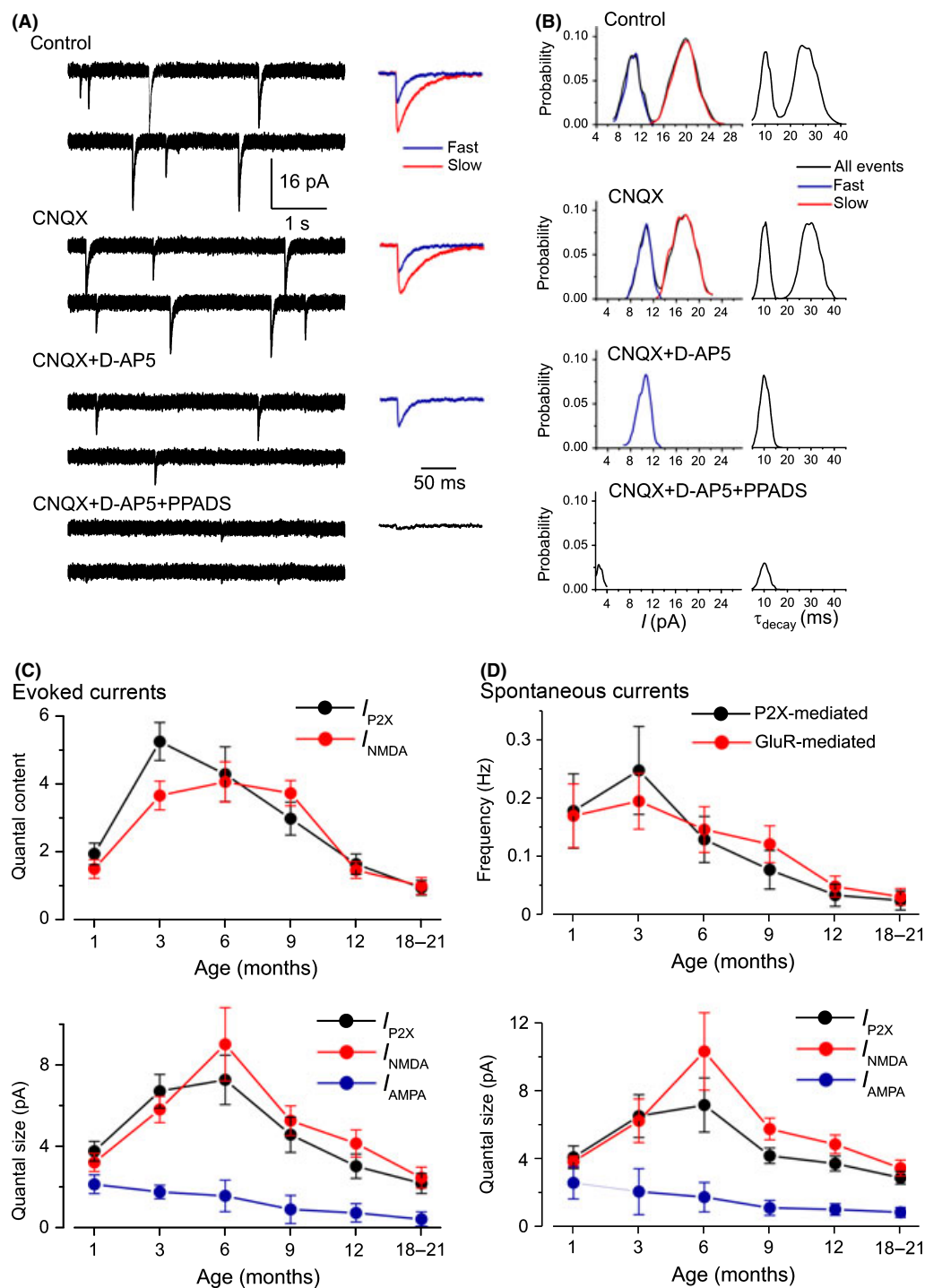


Fig. 4 Miniature spontaneous currents (mGSCs) in astrocytes *in situ* in cortical slices are mediated by the P2X, AMPA and NMDA receptors. (A) Representative whole-cell recordings from the cortical astrocyte of 6-month-old mouse in control and after consecutive application of 50 μ M CNQX, 30 μ M D-AP5 and 10 μ M PPADS. The right panels represent averaged waveforms of mGSCs (25 events). (B) Corresponding histograms for amplitude (left column) and decay time (right column) distribution of mGSCs. Fast mGSCs are indicated by blue lines; slow mGSCs are shown in red. Note the fast and slow mGSCs correspond to different peaks in the amplitude histograms. Antagonists of AMPA and NMDA receptors selectively inhibited slow currents, while PPADS selectively inhibited fast currents. These results indicate activation of two separate populations of purinergic and glutamatergic mGSCs. (C) Quantal analysis shows the age-related changes in the mean quantal content and quantal size of pharmacologically isolated P2X, NMDA and AMPA receptor-mediated evoked GSCs. Data are presented for 6–8 cells for each age. Statistical significance of difference between values of quantal content at 1 month and quantal content at 3, 6 and 9 months $P < 0.01$ (ANOVA); statistical significance of difference in the quantal size $P < 0.02$. (D) Age-related changes in the frequency and unitary size of spontaneous miniature synaptic currents in the cortical astrocytes. Data presented for 6–11 cells for each age. Note the consistent changes in the quantal size of evoked GSCs and unitary size of mGSCs. Statistical significance of difference in the mGSCs frequency at 1 month and all other ages $P < 0.02$ for both purinergic and glutamatergic currents; statistical significance of difference in the quantal size at 1, 3 and 6 months $P < 0.05$.

areas exposed to small but long-lasting elevations in concentration of neurotransmitters spilled out of the synaptic cleft. The contribution of both P2X and NMDA receptors to the slow component may be attributed to the high affinity of these receptors to ATP and glutamate and their slow desensitization (Lalo et al., 2006, 2008).

The age-dependent remodelling of astroglial synaptic responses may reflect changes in the release of neurotransmitters and/or changes in the density/efficacy of astroglial receptors. The underlying mechanisms can be determined by analysis of the quantal size of GSCs (directly related to the activity of postsynaptic receptors) and by analysis of the mean quantal content (which is indicative for changes in the neurotransmitter release). At the stimulation strength used, both the fast component of evoked GSCs and neuronal synaptic response exhibited similar large fluctuations, which enabled evaluation of the quantal parameters of pharmacologically isolated purinergic and glutamatergic GSCs (Fig. 4C) using quantal basic analysis techniques.

The quantal content of evoked purinergic GSCs increased between 1 and 3 months and then steadily declined. The quantal content of glutamatergic GSCs was much smaller in young age but exhibited considerable and sustained increase towards the mid-life and then a sharp decrease in the old age (Fig. 4C). Quantal size of both P2X and NMDA receptor-mediated GSCs had a similar behaviour with significant increase at 3 and 6 months old animals, which followed by substantial decrease at older ages. Quantal size of the AMPA receptor-mediated GSCs was maximal at 1 month and was steadily decreasing at later ages.

These results suggest that the strength of fast ionotropic signalling in cortical astrocytes reaches its peak at the early adulthood and then begins to decline. This was further corroborated by analysis of spontaneous GSCs (Fig. 4D). The frequency of mGSCs was higher at younger ages reaching maximum at 3 months and then steadily declined. The unitary size of P2X receptor-mediated mGSCs was increasing until 6 months and decreased significantly afterwards. The unitary size of NMDA receptor-mediated mGSCs was maximal at 6 months and decreased at older age. The unitary size of the AMPA receptor-mediated sGSCs was maximal in very young animals and declined significantly with aging.

Age-dependent changes in agonist-evoked currents in acutely isolated astrocytes

The data described earlier suggest age-dependent changes in the expression of ionotropic receptors in cortical astrocytes. This was directly confirmed in voltage-clamp experiments on astrocytes acutely isolated from the cortices of animals of different ages. In isolated cells, glutamate (100 μ M) typically triggered biphasic current responses (Fig. 5A). Application of the NMDA receptor antagonist D-AP5 (10 μ M) selectively reduced the steady-state component but did not affect the fast portion of the response. This latter was selectively inhibited by CNQX (30 μ M). The residual sustained component of the glutamate-induced current was completely blocked by the TBOA-mix in all cells tested. Applications of NMDA and ATP (Fig. 5A) triggered current responses that were completely blocked by D-AP5 (10 μ M) and PPADS (100 μ M), respectively. The ATP responses

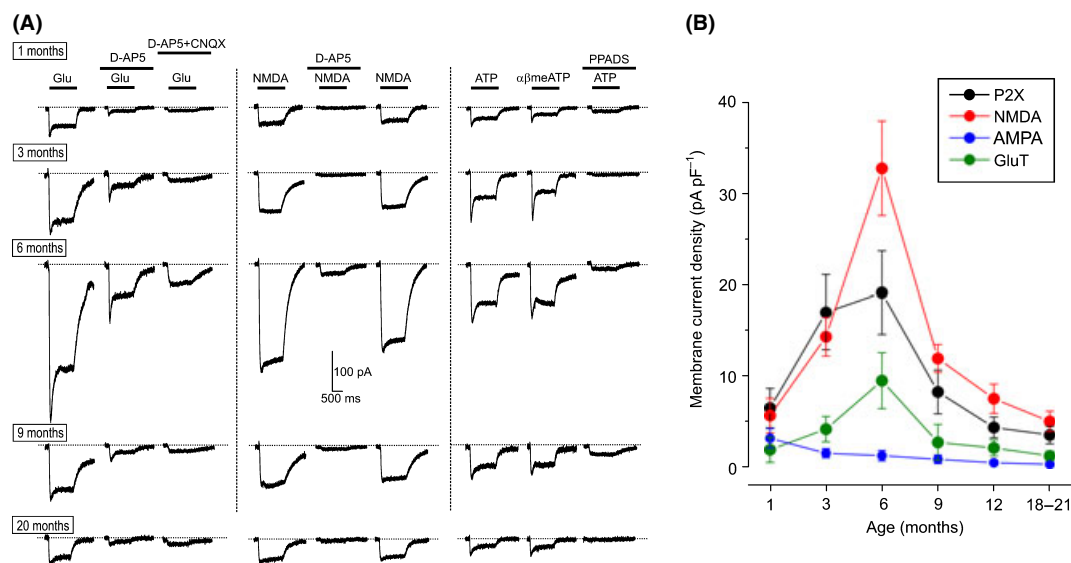


Fig. 5 Aging affects the density of glutamate transporter and ionotropic-receptor-mediated currents in acutely isolated single cortical astrocytes. (A) Representative whole-cell currents elicited in the acutely isolated astrocytes by application of 100 μ M glutamate (left column), 10 μ M NMDA (middle column) and 10 μ M ATP/ $\alpha\beta$ meATP at holding potential of -80 mV. Glutamate- and NMDA-evoked currents were inhibited by 10 μ M D-AP5 and 30 μ M CNQX; ATP-evoked currents were inhibited by 10 μ M PPADS. (B) The density of currents mediated by P2X, NMDA and AMPA receptors and glutamate transporters in cortical astrocytes (mean \pm SD for 9–12 cells for each age group); statistical significance of difference between average value for 1 month and corresponding values for ten and 6 months $P < 0.02$ (ANOVA) for all types of currents.

were also fully mimicked by P2X_{1/3} specific agonist $\alpha\beta$ -methylene ATP ($\alpha\beta$ meATP). Pharmacological properties of the agonist-evoked currents did not change with age and were consistent with properties of astroglial receptors previously described in young animals (Lalo *et al.*, 2006, 2008). Instead, aging significantly affected the amplitudes of responses to ATP, NMDA, AMPA and glutamate.

We observed a 3-fold and 6-fold increase in the density of P2X and NMDA receptor-mediated currents in isolated astrocytes in the adult age (Fig. 5). Both P2X and NMDA receptor-mediated currents were maximal at 6 months, which was followed by considerable decline at older ages. The density of AMPA-receptor-mediated currents was maximal at 1 month and gradually declined with age. These data agree with age-related changes of the astrocytic GSCs measured *in situ*. The density of glutamate-transporter-mediated current (recorded in the presence of CNQX and D-APV) also increased at 3 and even more at 6 months contrasting to the decrease in the transporter-mediated component of slow GSCs *in situ* (Fig. 5B). This may be explained by much lower density of transporter-mediated currents compared with NMDA and P2X currents at all ages (Fig. 5B); hence, the relative contribution of transporters to GSCs was smaller at the advanced ages.

Age-dependent changes in ionotropic-receptor-mediated astroglial Ca²⁺ signals

We recorded calcium signals in protoplasmic cortical astrocytes triggered by synaptic stimulation of ionotropic receptors (Fig. 6A). Slices incubation with selective AMPA receptor blocker CNQX (30 μ M) did not affect Ca²⁺ transients ($n = 8$, data not shown). In contrast, NMDA receptor blocker D-AP5 (30 μ M) and selective inhibitor of P2X_{1/5} receptors NF449 (10 nM) partially inhibited Ca²⁺ responses in all 14 astrocytes tested. The relative contribution of NMDA and P2X receptors to shaping Ca²⁺ signals changes with age (Fig. 6B), following the general pattern of changes in the GSC and agonist activated currents. The amplitudes of ionotropic-receptor-mediated Ca²⁺ signals were maximal at 3 and 6 months and decreased significantly at advanced ages (Fig. 6B).

Discussion

In this report, we demonstrated the age-dependent modification of synaptic transmission onto protoplasmic astrocytes in the neocortical structures. Neuronal activity evokes glial currents generally similar to postsynaptic currents in neurones, thus indicating that the astroglial membrane acts as a postsynaptic compartment. Astrocytes receive fast quantal signals, which most likely originate from vesicular release of glutamate and ATP from the presynaptic terminals. In addition to fast currents, astrocytes also possess slow synaptically activated currents mediated by glutamate transporters. Fast GSCs were apparently evoked in areas of astroglial membrane exposed to high concentrations of glutamate as part of this component

was mediated by astrocytic AMPA receptors with relatively low glutamate sensitivity (Lalo *et al.*, 2006). These astroglial compartments may surround or even protrude into the synaptic cleft (Volterra & Meldolesi, 2005; Fiacco *et al.*, 2009) or may be a direct target of axon collaterals, like synapses on NG-2 glial cells (Paukert & Bergles, 2006). Slow GSCs are generated in the areas exposed to small but long-lasting elevations in concentration of neurotransmitters (probably because of the spillover of the neurotransmitter from the synaptic cleft) as suggested by the lack of CNQX sensitivity and significant contribution of high-affinity NMDA receptors and glutamate transporters.

The role of ectopic neurotransmitter release in inducing GSC in the cortex remains doubtful. Indeed in our previous experiments in the young mice (Lalo *et al.*, 2006), we found that cyclothiazide (CTZ; a compound that increases the apparent affinity of AMPA receptors (Yamada & Tang, 1993; Partin *et al.*, 1994)) increases AMPA-mediated component of glial synaptically activated current by 96%, which is in a good agreement with effect of CTZ on neuronal synaptic currents (Yamada & Tang, 1993). Such an increase in astroglial currents also closely resembles a twofold increase in the amplitude of response of the climbing fibre synapses on NG-2 glial cells in cerebellum (Lin *et al.*, 2005). In contrast, currents activated in the Bergmann glia following ectopic release exhibited more than eightfold increase under CTZ because of exposure of glial AMPA receptors to low concentrations of glutamate (Dzubay & Jahr, 1999). Additional similarity of cortical GSCs in young mice to synaptically activated currents in the NG-2 cells (Paukert & Bergles, 2006) is their sustainability at repetitive stimulation (we could record GSCs for more 40–60 min at 0.3–0.5 Hz – see Fig. 2B), whereas glial currents activated by ectopic release fade rapidly because of pre-synaptic depression and fast depletion of ectopic transmitter pools (Matsui & Jahr, 2004; Paukert & Bergles, 2006). The GSCs recorded in old animals are much more susceptible to the depression at high stimulation frequency, which may be explained by re-modelling of the neuron-driven input onto astrocytes that may include an increased contribution of ectopic release. Alternatively, the synaptic fatigue may develop faster in old animals, leading to the use-dependent decrease in neurotransmitter release.

Glial synaptic responses were modified through the maturation and aging of the brain. The age-related changes in the GSCs amplitude cannot be attributed to changes in the astrocytes input resistance. First, increase in GSC amplitudes recorded in 3 and 6 months was accompanied by decrease in the input resistance (which would decrease the current measured at soma). Second, changes in the input resistance in astrocytes in three- and 6-months-old animals were rather minor. Using the cable theory of whole-cell voltage-clamp recording *in situ* (Major *et al.*, 1993), it is possible to estimate that 30% change in the input resistance may account for only 3–4% change in the amplitude of current measured at soma in our experimental conditions (the series/input resistance ratio of 8–15).

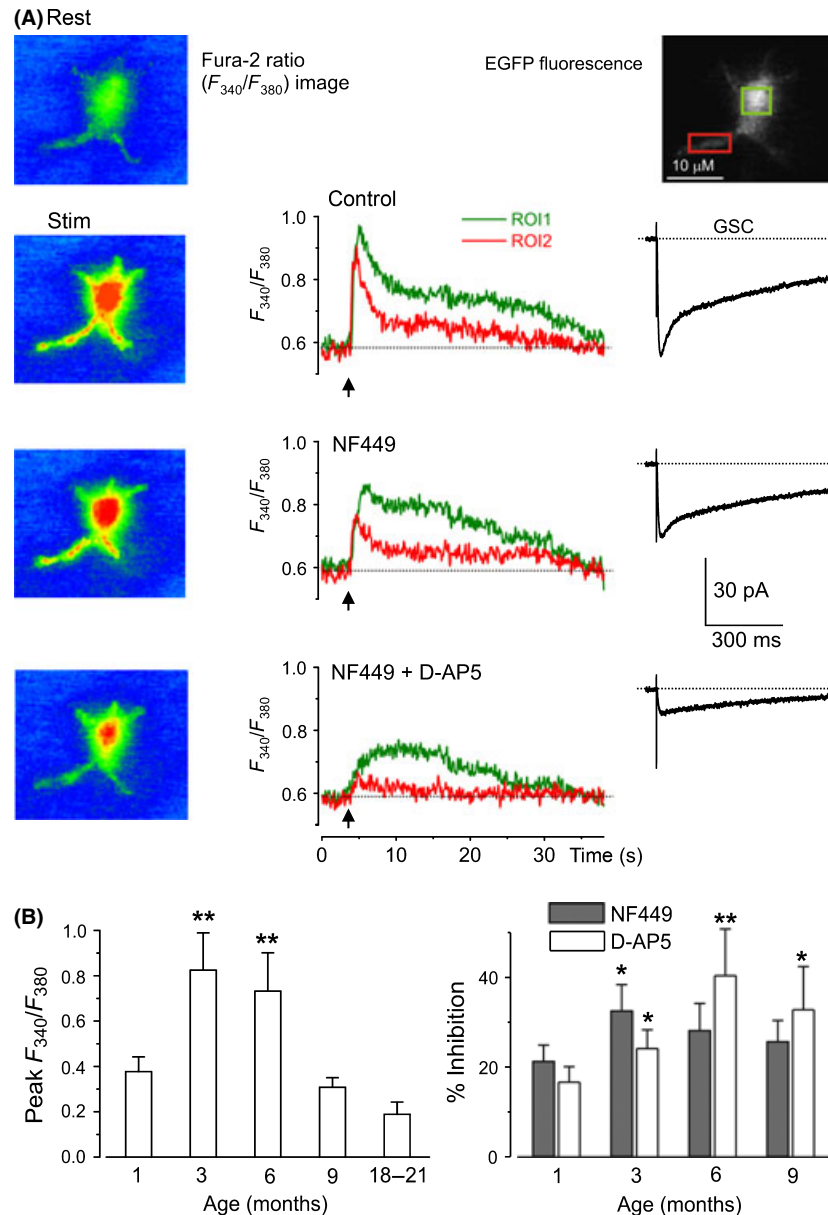


Fig. 6 Age-dependent changes in synaptically induced ionotropic Ca^{2+} signals in protoplasmic astrocytes *in situ* in cortical slices. (A) Cortical layer II astrocyte of 9-month-old mouse was loaded with Fura-2 *in situ* via patch pipette. Fluorescent images were recorded simultaneously with glial currents evoked by neuronal afferent stimulation in presence of TBOA-mix and CNQX (control) and after consecutive application of 10 nM NF-449 (selective antagonist of P2X receptors) and 30 μM D-AP5. Representative images (pseudo-colour, pipette image subtracted) and glial synaptic currents (right column) were recorded before (rest) and after stimulation as indicated. Ca^{2+} -transients (middle column) are expressed as F_{340}/F_{380} ratio averaged over the corresponding regions of interest shown in the glial fibrillary acidic protein image of astrocyte (top right). (B) Age-related changes in the astrocytic Ca^{2+} -signalling. *Left panel*, average peak amplitudes of $[\text{Ca}^{2+}]_i$ increases induced by stimulation of neuronal afferents in cortical astrocytes of different ages. *Right panel*, average inhibitory effect of antagonists of P2X (NF449) and NMDA (D-AP5) receptors on the amplitudes of $[\text{Ca}^{2+}]_i$ increases responses in cortical astrocytes. Data are presented as mean \pm SD for 3–4 cells for each age group; * $P < 0.05$, ** $P < 0.01$ one-way ANOVA compared with 1 month.

In young animals, the synaptic glial responses were relatively small; in the course of CNS maturation, they increased several times, mostly because of the increase in the density of NMDA and P2X receptors (Fig. 5). The maximal strength of glial synaptic responses was attained at 6 month. Further increase in age resulted in the decrease in the density of ionotropic receptors and overall diminution of astroglial synaptic currents. Importantly, the considerable decrease in the ampli-

tude of the synaptically driven currents in old age (Fig. 3C) originates both from decrease in the density of ionotropic receptors, as indicated by the diminution of the quantal size of evoked and spontaneous GSCs, and decline in the release of glutamate and ATP from neurones onto glial cells, manifested by substantial decrease in the quantal content of evoked GSCs and the frequency of spontaneous currents (Fig. 4C,D).

Glutamate transporters do not seem to play a major role in astroglial ionotropic signalling, especially at three and 6 months, most likely due their lower efficiency in the electric charge transfer per single glutamate molecule bound. The major role for transporters seems to be clearing glutamate from extracellular space and increase in their density at three and 6 months most probably reflects the homeostatic response to the increased release of glutamate (as could be postulated based on the analysis of quantal content). We also found that NMDA and P2X receptors provide significant Ca^{2+} influx in the astrocytes which is subjected to age-dependent remodelling.

Naturally, our results offer a wide and open field for speculations, indicating for example an age-dependent decrease in synaptic communication in neuronal-glia circuitry that may in turn signify the beginning of age-dependent decline in brain functions; alternatively, however, the bell-shaped changes in glial synaptic transmission may reflect maturation of the CNS, pruning of functionally irrelevant synaptic contacts and manifest the 'attainment of wisdom' which generally accompanies advanced age.

Acknowledgments

Authors research was supported by BBSRC (BB/F021445 to YP) and by Grant Agency of the Czech Republic (GACR 305/08/1381 and GACR 305/08/1384 to AV).

References

- Araque A, Parpura V, Sanzgiri RP, Haydon PG (1999) Tripartite synapses: glia, the unacknowledged partner. *Trends Neurosci.* **22**, 208–215.
- Bergles DE, Roberts JD, Somogyi P, Jahr CE (2000) Glutamatergic synapses on oligodendrocyte precursor cells in the hippocampus. *Nature* **405**, 187–191.
- Bezzi P, Domercq M, Vesce S, Volterra A (2001) Neuron-astrocyte cross-talk during synaptic transmission: physiological and neuro-pathological implications. *Prog. Brain Res.* **132**, 255–265.
- Danbolt NC (2001) Glutamate uptake. *Progr. Neurobiol.* **65**, 1–105.
- Dzubay JA, Jahr CE (1999) The concentration of synaptically released glutamate outside of the climbing fiber-Purkinje cell synaptic cleft. *J. Neurosci.* **19**, 5265–5274.
- Fellin T, Pozzan T, Carmignoto G (2006) Purinergic receptors mediate two distinct glutamate release pathways in hippocampal astrocytes. *J. Biol. Chem.* **281**, 4274–4284.
- Fiocco TA, Agulhon C, McCarthy KD (2009) Sorting out astrocyte physiology from pharmacology. *Annu. Rev. Pharmacol. Toxicol.* **49**, 151–174.
- Grass D, Pawlowski PG, Hirrlinger J, Papadopoulos N, Richter DW, Kirchhoff F, Hulsman S (2004) Diversity of functional astroglial properties in the respiratory network. *J. Neurosci.* **24**, 1358–1365.
- Halassa MM, Fellin T, Haydon PG (2007) The tripartite synapse: roles for gliotransmission in health and disease. *Trends Mol. Med.* **13**, 54–63.
- Haydon PG (2001) GLIA: listening and talking to the synapse. *Nat. Rev. Neurosci.* **2**, 185–193.
- Haydon PG, Carmignoto G (2006) Astrocyte control of synaptic transmission and neurovascular coupling. *Physiol. Rev.* **86**, 1009–1031.
- Hu WH, Walters WM, Xia XM, Karmally SA, Bethea JR (2003) Neuronal glutamate transporter EAAT4 is expressed in astrocytes. *Glia* **44**, 13–25.
- Lalo UV, Pankratov YV, Arndts D, Krishtal OA (2001) Omega-conotoxin GVIA potently inhibits the currents mediated by P2X receptors in rat DRG neurons. *Brain Res. Bull.* **54**, 507–512.
- Lalo U, Pankratov Y, Kirchhoff F, North RA, Verkhratsky A (2006) NMDA receptors mediate neuron-to-glia signaling in mouse cortical astrocytes. *J. Neurosci.* **26**, 2673–2683.
- Lalo U, Pankratov Y, Wichert SP, Rossner MJ, North RA, Kirchhoff F, Verkhratsky A (2008) P2X₁ and P2X₅ subunits form the functional P2X receptor in mouse cortical astrocytes. *J. Neurosci.* **28**, 5473–5480.
- Lin SC, Huck JH, Roberts JD, Macklin WB, Somogyi P, Bergles DE (2005) Climbing fiber innervation of NG2-expressing glia in the mammalian cerebellum. *Neuron* **46**, 773–785.
- Major G, Evans JD, Jack JJ (1993) Solutions for transients in arbitrarily branching cables: II. Voltage clamp theory. *Biophys. J.* **65**, 450–468.
- Matsui K, Jahr CE (2004) Differential control of synaptic and ectopic vesicular release of glutamate. *J. Neurosci.* **24**, 8932–8939.
- Matthias K, Kirchhoff F, Seifert G, Huttman K, Matyash M, Kettenmann H, Steinhauser C (2003) Segregated expression of AMPA-type glutamate receptors and glutamate transporters defines distinct astrocyte populations in the mouse hippocampus. *J. Neurosci.* **23**, 1750–1758.
- Nolte C, Matyash M, Pivneva T, Schipke CG, Ohlemeyer C, Hanisch UK, Kirchhoff F, Kettenmann H (2001) GFAP promoter-controlled EGFP-expressing transgenic mice: a tool to visualize astrocytes and astrogliosis in living brain tissue. *Glia* **33**, 72–86.
- Pankratov YV, Krishtal OA (2003) Distinct quantal features of AMPA and NMDA synaptic currents in hippocampal neurons: implication of glutamate spillover and receptor saturation. *Biophys. J.* **85**, 3375–3387.
- Pankratov Y, Lalo U, Krishtal O, Verkhratsky A (2002) Ionotropic P2X purinoreceptors mediate synaptic transmission in rat pyramidal neurones of layer II/III of somato-sensory cortex. *J. Physiol.* **542**, 529–536.
- Pankratov Y, Lalo U, Verkhratsky A, North RA (2007) Quantal release of ATP in mouse cortex. *J. Gen. Physiol.* **129**, 257–265.
- Partin KM, Patneau DK, Mayer ML (1994) Cyclothiazide differentially modulates desensitization of alpha-amino-3-hydroxy-5-methyl-4-isoxazolepropionic acid receptor splice variants. *Mol. Pharmacol.* **46**, 129–138.
- Paukert M, Bergles DE (2006) Synaptic communication between neurons and NG2+ cells. *Curr. Opin. Neurobiol.* **16**, 515–521.
- Rettinger J, Braun K, Hochmann H, Kassack MU, Ullmann H, Nickel P, Schmalzing G, Lambrecht G (2005) Profiling at recombinant homomeric and heteromeric rat P2X receptors identifies the suramin analogue NF449 as a highly potent P2X₁ receptor antagonist. *Neuropharmacology* **48**, 461–468.
- Stricker C, Field AC, Redman SJ (1996) Statistical analysis of amplitude fluctuations in EPSCs evoked in rat CA1 pyramidal neurones *in vitro*. *J. Physiol.* **490** (Pt 2), 419–441.
- Verkhratsky A, Kirchhoff F (2007) NMDA receptors in glia. *Neuroscientist* **13**, 28–37.
- Verkhratsky A, Orkand RK, Kettenmann H (1998) Glial calcium: homeostasis and signaling function. *Physiol. Rev.* **78**, 99–141.
- Volterra A, Meldolesi J (2005) Astrocytes, from brain glue to communication elements: the revolution continues. *Nat. Rev. Neurosci.* **6**, 626–640.
- Yamada KA, Tang CM (1993) Benzothiadiazides inhibit rapid glutamate receptor desensitization and enhance glutamatergic synaptic currents. *J. Neurosci.* **13**, 3904–3915.